

一种新型二氰基乙烯修饰的二呋喃环戊烯光开关: 荧光性质、 传感性能和生物应用

郑天骄^a 陈炫颖^a 朱亮亮^c 王道累^a
邹祺^{*a} 曾涛^{*b} 陈文博^{*a}

^a 上海电力大学 上海市电力材料防护与新材料重点实验室 上海 200090)

^b 上海市材料研究所 上海市工程材料应用与评价重点实验室 上海 200437)

^c 复旦大学高分子科学系 聚合物分子工程国家重点实验室 上海 200438)

摘要 近年来,借助于高度优化的小分子荧光染料,荧光蛋白和先进的标记技术,荧光标记技术得到了极大的发展.二芳基乙烯光开关荧光染料的研究,主要通过二芳基乙烯中引入荧光核和对芳基的结构修饰.与噻吩相比,呋喃具有更好的刚性、溶解性和可生物降解能力以及更强的荧光.因此,二呋喃乙烯可以作为荧光标记技术的小分子荧光染料.设计并制备了一种基于二氰基乙烯的二呋喃乙烯新型荧光光开关.该化合物在溶液中呈现典型的可逆光致变色性能,且以其出色的选择性、灵敏度和高对比度来实现氰根离子的荧光检测.此外,通过核磁滴定实验,解释了其对氰根离子的响应机理.由于采用呋喃替换噻吩使得该化合物拥有更强的荧光,成功应用于生物体内的荧光染料和氰根离子探针.

关键词 二呋喃乙烯; 光开关; 荧光检测; 氰化物; 生物成像

A New Dicyano-vinyl Modified Difurylperhydrocyclopentene Photoswitch: Fluorescent Properties, Sensing Ability and *in vivo* Application

Zheng, Tianjiao^a Chen, Xuanying^a Zhu, Liangliang^c Wang, Daolei^a
Zou, Qi^{*a} Zeng, Tao^{*b} Chen, Wenbo^{*a}

^a Shanghai Key Laboratory of Materials Protection and Advanced Materials in Electric Power, Shanghai University of Electric Power, Shanghai 200090)

^b Shanghai Key Laboratory of Engineering Materials Application and Evaluation, Shanghai Research Institute of Materials, Shanghai 200437)

^c State Key Laboratory of Molecular Engineering of Polymers, Department of Macromolecular Science, Fudan University, Shanghai 200438)

Abstract Recently, fluorescent labeling techniques have been greatly developed with the aid of highly optimized small-molecule fluorescent dyes, fluorescent proteins and advanced tagging techniques. Many reasonable strategies have been used to design fluorescent diarylethene, mainly focusing on the introduction of luminophores by conjugated junction and the modification of aryl cores in the diarylethene. Compared to thiophene, furan has superior properties such as solubility, biodegradable ability and rigidity fluorescence. Therefore, difurylethene is a better candidate for fluorescent labeling techniques. Herein, a new fluorescent photoswitch based on dicyano-vinyl modified difurylethenes was designed and prepared. This compound demonstrates typical reversible photochromism in solution and outstanding performance for the fluorescent detection of cyanide ions with excellent selectivity, sensitivity and high contrast. Furthermore, the mechanism of sensing toward cyanide ions was explained by ¹H NMR titrations experiments. Owing to the strong fluorescence from a superior derivation with furan

* Corresponding authors. E-mail: zqou@shiep.edu.cn; zengtao0626@126.com; wenbochen@shiep.edu.cn

Received March 17, 2019; revised April 22, 2019; published online May 6, 2019.

Project supported by the National Natural Science Foundation of China (Nos. 21406137, 61502297), the Natural Science Foundation of Shanghai City (No. 17ZR1447100), and the Science and Technology Commission of Shanghai Municipality (No. 14DZ2261000).

国家自然科学基金(Nos. 21406137, 61502297)、上海市自然科学基金(No. 17ZR1447100)和上海市科学技术委员会(No. 14DZ2261000)资助项目.

instead of thiophene, it is successfully applied as the fluorescent dyes and probe for detecting cyanide ions in vivo application.

Keywords difurylperhydrocyclopentene; photoswitch; fluorescent detection; cyanide; bioimaging

1 Introduction

Fluorescent labeling techniques have been greatly developed recently with the aid of highly optimized small-molecule fluorescent dyes,^[1-7] fluorescent proteins^[8] and advanced tagging techniques.^[9] Among small-molecule fluorescent dyes, the photoswitching molecules possibly alternate between two different fluorescent states. This makes them to be one of the most ideal candidates for the optical microscopy, especially super-resolution microscopy,^[10] enabling cellular optical imaging with spatial resolution beyond the classical diffraction limit.^[11,12] As the typical photoswitches, diarylethene derivatives (DAE), particularly, the substituted bis(heteroaryl)-cycloalkenes are one of the most promising families because of their excellent structural modifications and remarkable thermal stability as well as rapid light response, *etc.*^[12-16] So far, many reasonable strategies have been used to design fluorescent DAE, mainly focusing on the introduction of luminophores by conjugated junction.^[17] However, the modified aryl cores in the DAE architectures to realize fluorescent emission mainly limited to thiophene heterocyclic analogues, such as benzothio- phene and benzothiophene 1,1-dioxide.^[18-22]

Compared to thiophene, furan and its derivatives have been less studied in DAEs for years. Infrequent furan-based DAEs that are chemically tailored by the central ethene bridges have been reported, suggesting comparable switching properties to dithienylethenes.^[23-28] Recent studies have shown that solubility, biodegradable ability and rigidity of optoelectrical materials can be improved by replacing thiophene with furan unit.^[29-35] Furthermore, furan derivatives tend to exhibit stronger fluorescence,^[36] suggesting promising candidates for the fluorescence labelling and sensing.

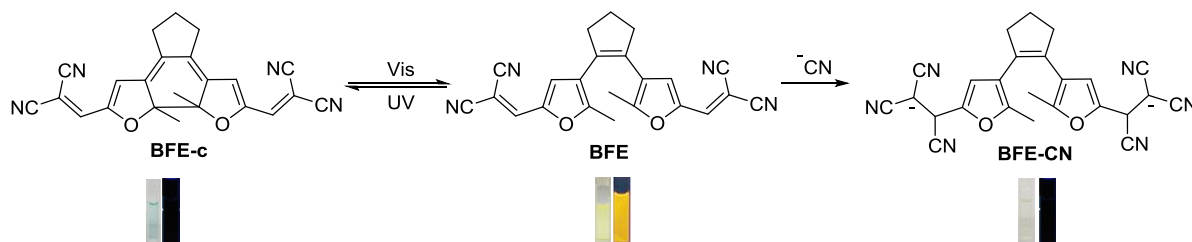
Recently, a new type of difurylperhydrocyclopentene prepared by classic reactions in mild conditions was reported, showing that furan is superior to thiophene with regard to fluorescence properties, photocyclization conversion yield, better fatigue resistance and no cytotoxicity.^[37] These results encouraged us to carry on the further structural modification of photochromic molecules on the strength of the furan moiety. Herein, a fluorescent photoswitch based on bisfurylethenes was subtly designed and facilely synthesized by the Knoevenagel condensation reaction. Compared to previous furan-based DAEs, this compound **BFE** as depicted in Scheme 1 exhibits red-shifted fluorescent emission, which is a better candidate to act as small-molecule fluorescent dyes for fluorescent labeling techniques. More importantly, this bisfurylethenes compound could serve as a photo-controlled chemodosimeter for cyanide ions with high selectivity, and was successfully applied in the bioimaging.

2 Results and discussion

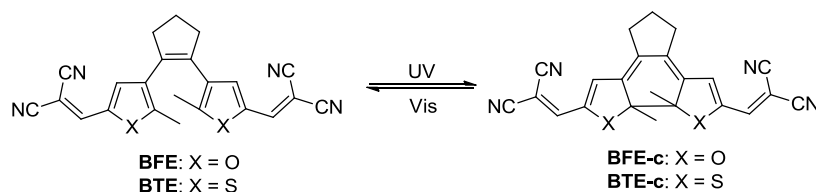
2.1 Photochromic behaviors and fluorescent studies

The photochromic behaviors of compound **BFE** (1×10^{-5} mol/L solution in acetonitrile) were studied at the room temperature and the corresponding analogue **BTE** was used as a reference compound under the same condition (Scheme 2). It was found that compound **BFE** displayed a classical photochromic behavior of diarylethene derivatives when it was alternately irradiated with ultraviolet and visible light.

Figure 1A demonstrated the spectral changes of the absorption of compound **BFE** in acetonitrile solution. It was found that compound **BFE** had a sharp absorption band at 386 nm. When irradiated with 365 nm light, there was a new absorption band coming up at 674 nm. Furthermore,



Scheme 1 Design strategy of compound **BFE** responsive to CN^- ions with photochromism



Scheme 2 Photochromic process of diarylethene derivatives alternately irradiated with ultraviolet and visible light

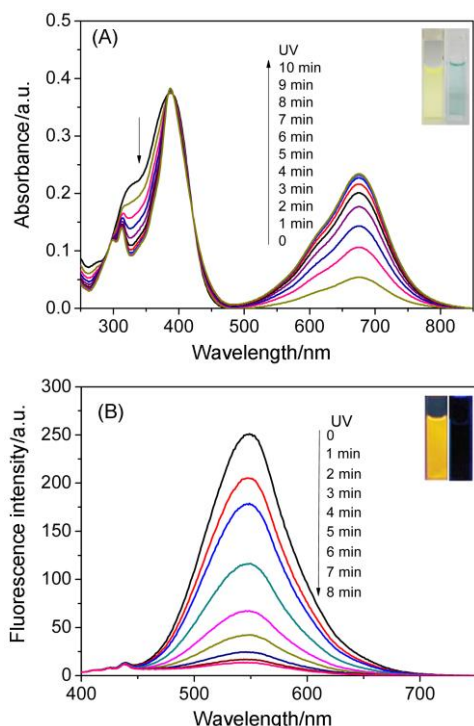


Figure 1 UV-vis absorption changes (A) and fluorescence changes (B) of compound **BFE** (10 $\mu\text{mol/L}$) in acetonitrile solution upon irradiation with 365 nm light at 25 $^{\circ}\text{C}$, $\lambda_{\text{ex}}=386$ nm. Slits: 5 nm/5 nm. Inset: the corresponding photographic images irradiated with UV and visible light, respectively

with the irradiation time prolongation, the intensity of 674 nm band increased rapidly till it reached to the photostationary state, indicating the formation of the closed-ring isomer (**BFE-c**) accompanied by the change of the solution colour from yellow to blue (Figure 1A inset). When irradiated with visible light (≥ 520 nm), the blue solution can restore to yellow and the absorption spectrum also returned to the original state, demonstrating the conversion of the ring-closed isomer to the ring-open isomer. In comparison with compound **BTE-c**, it was found that the absorption maximum of compound **BFE-c** was shorter about 22 nm in acetonitrile solution. But the absorption maximum of compound **BFE-c** red-shifted about 152 nm compared to that of reported aldehyde-based difurylperhydrocyclopentene **1**^[37] at the photostationary state due to the better conjugated structure of compound **BFE**.

The emission peak at around 547 nm for compound **BFE** was also observed when it was excited at 386 nm (Figure 1B) and its emission also exhibited a good response to UV light. When irradiated with 365 nm light, the green fluorescence of compound **BFE** was gradually quenched with the increase of the irradiation time till there was no fluorescence at the photostationary state (Figure 1B inset). And its fluorescence can be restored to the original emission intensity when irradiated with visible light (≥ 520 nm). The fluorescence quantum yield of compound **BFE** was determined to be 0.939% in acetonitrile and its fluorescence lifetimes was 0.7 ns. Compound **BTE** showed

no fluorescence due to the less flexibility of furan ring, whereas the thiophene ring affected the non-radiative process.^[26,37] Impressively, the emission of compound **BFE** red-shifted around 75 nm relative to that of compound **1** due to the strong ICT effect derived from cyano groups to bisfurylethene core in the molecule **BFE**.

The thermal irreversibility is the important property for the diarylethene-based photoswitches, especially the thermal stability of closed-ring forms at higher temperature.^[38,39] The thermal-stability experiments were conducted in refluxed toluene under argon atmosphere. It was observed that the closed-ring form of compound **BTE** exhibited good thermal stability up to 110 $^{\circ}\text{C}$ in toluene with an extended time of 2 h. For compound **BFE**, its closed-ring form was much stable under the same conditions, and faded within 3 h. Therefore, compound **BFE** showed better thermal stabilities than **BTE**.

2.2 Colorimetric and fluorescent response to cyanide

The absorption spectra changes of compound **BFE** were firstly studied when the solution of aqueous CN^- was gradually added. As depicted in Figure 2A, there were two major absorption bands centered at 220 and 386 nm, respectively, in the UV-vis absorption spectra of compound **BFE**. The 386 nm absorption band decreased with the gradual addition of CN^- and finally disappeared when the amounts of CN^- increased to 2.2 equiv. Meanwhile, the absorption band at 220 nm grew up with an isosbestic point at 274 nm. This observation provided the evidence of

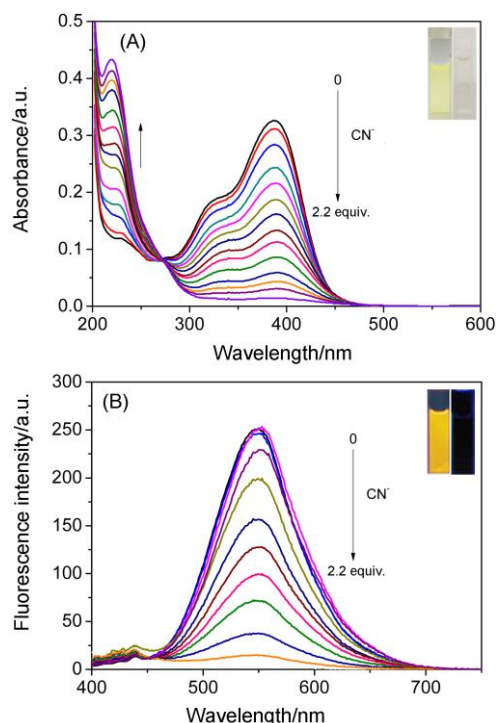


Figure 2 UV-vis absorption (A) and fluorescence (B) spectral changes of compound **BFE** (10 $\mu\text{mol/L}$) in the presence of an increased concentration of CN^- (0~22 $\mu\text{mol/L}$) in acetonitrile solution at 25 $^{\circ}\text{C}$ ($\lambda_{\text{ex}}=386$ nm, slits: 5 nm/5 nm)

the intramolecular charge transfer (ICT) effect occurred during the CN^- titration.

Then the effect of CN^- concentration change on the fluorescence spectra of compound **BFE** was further explored. As demonstrated in Figure 2B, there was a strong fluorescence band centred around 548 nm in the fluorescence spectra of compound **BFE**, due to the ICT involved in electron-donor group (difurylperhydrocyclopentene core) and electron-withdrawing groups (dicyano-vinyl).^[40–44] The fluorescence emission centred at 548 nm decreased dramatically when gradually adding CN^- to the solution of compound **BFE** and the fluorescence was completely quenched when the amount of CN^- reached 2.2 equiv. The inset graph in Figure 2B demonstrated that the naked eye could easily discriminate the two fluorescence states by simply using a handle UV lamp.

The ^1H NMR titration experiments (in $\text{CH}_3\text{CN}-d_3$) of the compound **BFE** was used to analyze the reaction mechanism (Figure 3). With the continuous addition of CN^- , the protons on the dicyano-vinyl group (H_1 and H_2) at δ 7.58 were gradually weakened and it disappeared when the CN^- concentration was 2.2 equiv., accompanied by the appearance and growth of a new peak (H_1'' and H_2'') around δ 4.40. This chemical shift of H_1'' and H_2'' was consistent with the dicyano-vinyl protons due to the nucleophilic addition of the cyanide toward the dicyano-vinyl group. Meanwhile, the protons on the furan ring (H_3 and H_4) shifted from δ 7.15 to 6.18, resulting from the decreased electron-withdrawing effect of the dicyano-vinyl groups. The ^1H NMR analysis indicated that the cyanide functioned as a nucleophile during the transformation from **BFE** to **BFE-CN**. Therefore, the disappearance of the emission peak should be ascribed to the nucleophilic addition of the equivalent CN^- to the electrophilic carbon atom of the $\text{C}=\text{C}$ bond of dicyano-vinyl group, which in turn suppresses the ICT effect, as shown in Scheme 1. Two electron-withdrawing dicyanidyl groups are converted to electron-rich anionic groups during the nucleophilic addition process, meanwhile, the $\text{C}=\text{C}$ double bond is broken and the negative charge simultaneously presents.

In Figure 4, the CN^- concentration-dependence of fluorescence intensity at 548 nm was plotted for better visualizing the sensing process. The fluorescence intensity decreased with the increase of CN^- concentration and became saturated when CN^- was at the concentration of 2.2 equiv. The inset of Figure 4 showed that the fluorescence intensity at 548 nm varied linearly with CN^- concentration from 4 $\mu\text{mol/L}$ to 20 $\mu\text{mol/L}$, suggesting a coefficient $R^2=0.9959$. Therefore, compound **BFE** can serve as a practical detector to calibrate and determinate CN^- concentration in acetonitrile solution.

Next, the sensing selectivity of compound **BFE** towards CN^- was also evaluated. Under the same conditions, the changes of absorption and fluorescence of compound **BFE** were tested when adding 10 different anions, such as F^- , Cl^- , Br^- , I^- , CH_3COO^- , CO_3^{2-} , NO_3^- , PO_4^{3-} , SO_3^{2-} and SO_4^{2-} . The ratio of absorption at 386 nm (A_1/A_0) at 386

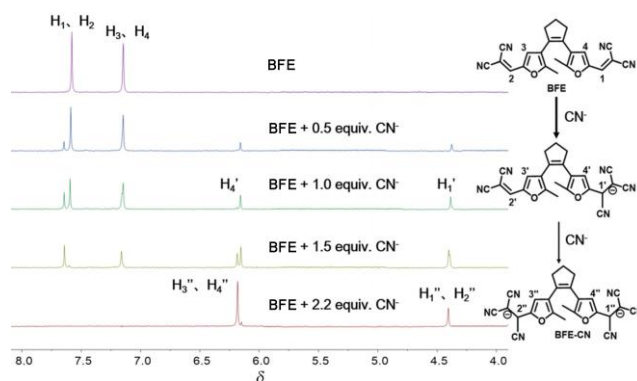


Figure 3 Partial ^1H NMR (400 MHz) titrations of the **BFE** in acetonitrile- d_3 with the addition of CN^- . Each spectrum was acquired 2 min after the addition of CN^- in acetonitrile- d_3 .

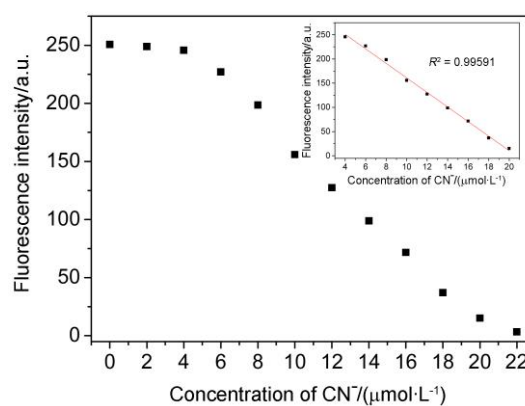


Figure 4 CN^- concentration-dependence of fluorescence intensity at 548 nm of compound **BFE** (10 $\mu\text{mol/L}$) in acetonitrile solution at 25 $^\circ\text{C}$ ($\lambda_{\text{ex}}=386$ nm, slits: 5 nm/5 nm). Inset: the fluorescence intensity at 548 nm as a linear function of CN^- concentration (4–20 $\mu\text{mol/L}$)

nm) before and after the addition of anions in acetonitrile were summarized and displayed in Figure 5A. The results showed that these competitive anions did not bring any significant change in the absorbance even at high concentration (20 equiv.). And Figure 5B summarized the fluorescence quenching efficiency of compound **BFE** at 548 nm, which was calculated by $(I_0-I)/I_0$, where I_0 and I described fluorescence intensity of compound **BFE** before and after adding anions respectively. It was found that only CN^- could result in the dramatic changes of the fluorescence quenching efficiency. These results suggest that CN^- could selectively bring about apparent color and fluorescent changes of compound **BFE**. Overall, compound **BFE** shows extraordinary sensing ability and selectivity to CN^- over other competitive anions under high concentrations, therefore it can be used as an efficient colorimetric and fluorescent probe to detect CN^- .

2.3 Bioimaging

To validate the effectiveness of compound **BFE** for the CN^- response in cellular imaging, HeLa cells were chosen as the example cell line and carry out the confocal laser scanning experiments. During these experiments, **BFE** and

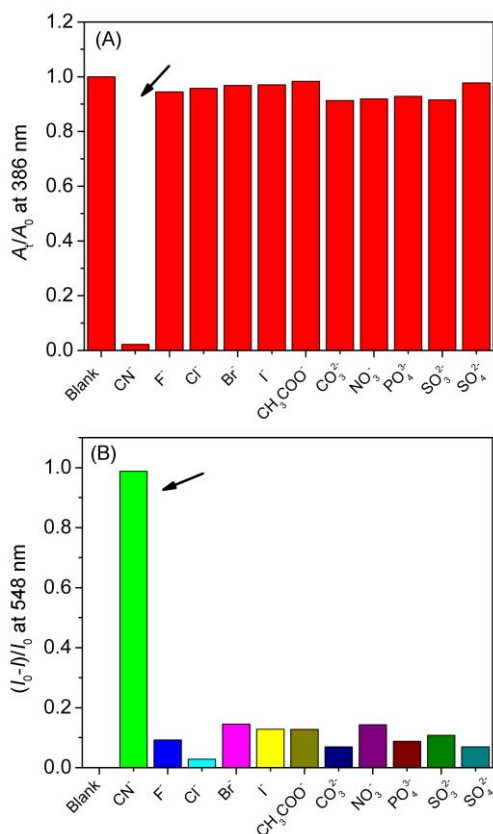


Figure 5 Ratio of absorption at 386 nm (A_i/A_0 at 386 nm) (A) and the fluorescence quenching efficiency ($(I_0 - I)/I_0$ at 548 nm) (B) of compound **BFE** (10 $\mu\text{mol/L}$) in the absence and presence of anions in acetonitrile at 25 $^\circ\text{C}$ ($\lambda_{\text{ex}}=357$ nm, slits: 5 nm/5 nm)

the corresponding photostationary state **BFE-c** were used as the imaging agents to avoid the harmful impact of UV irradiation on living cells. As the reference, the photochromic properties of compound **BFE** and its response to CN^- in dimethyl sulfoxide (DMSO) solution were also tested. Compound **BFE** showed good properties in DMSO solution. **BFE** (10 $\mu\text{mol/L}$) in RPMI-1640/DMSO ($V:V=99:1$) was employed for the treatment of the HeLa cells for 30 min at 37 $^\circ\text{C}$ and a bright green fluorescence was observed in the fluorescence images (Figures 6A and 6C). Under the same conditions, the incubation of **BFE-c** exhibited very weak fluorescence (Figures 6D and 6F), which agreed with the observations showed in Figure 1B. Compared with **BFE-c**, the imaging of **BFE**-treated HeLa cells showed strong fluorescence. More importantly, there were no any gross morphological changes in the bright field images of cells incubated with **BFE** and **BFE-c**, indicating that cells were viable during the whole imaging experiments. To further assess the feasibility of compound **BFE** for biological applications as a probe, the corresponding cellular imaging experiments with CN^- were also performed. In the growth medium, cells were treated with 20 $\mu\text{mol/L}$ CN^- for 20 min at 37 $^\circ\text{C}$, and then incubated with compound **BFE** for 30 min at 37 $^\circ\text{C}$. The intracellular region exhibited arresting switch-OFF fluores-

cence in the cellular imaging experiments (Figures 6G and 6I). Furthermore, the overlay of fluorescence and bright-field images demonstrated that fluorescence signals were localized in the cytosol region, indicating the efficient permeation of compound **BFE** through the living cells from the growth medium. These results were consistent with the observations in titration experiments (Figure 2B). To confirm whether some reductive substances in cells disturbed the detection, the interaction of cysteine and glutathione with compound **BFE** in DMSO solution were studied. It was observed that the ultraviolet absorption and fluorescence emission spectra of compound **BFE** did not change significantly after adding 2.2 equiv. of cysteine and glutathione, respectively. Therefore, based on the appropriate structural modification of bisfurylene, compound **BFE** shows strong fluorescence and “on-off” responses to UV light and CN^- in cell imaging, suggesting that compound **BFE** can work as a multifunctional fluorescent switch to readily monitor CN^- for biological applications.

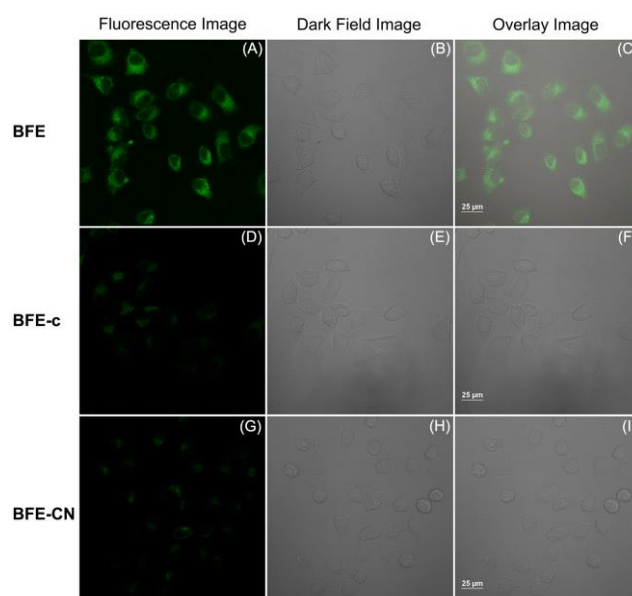


Figure 6 Confocal fluorescence and bright-field images of living HeLa cells

(A) Fluorescence image, (B) bright-field image, and (C) the overlay image of HeLa cells incubated with **BFE** (10 $\mu\text{mol/L}$) in the growth media for 30 min at 37 $^\circ\text{C}$. (D) Fluorescence image, (E) bright-field image, and (F) the overlay image of HeLa cells incubated with **BFE-c** (10 $\mu\text{mol/L}$) in the growth media for 30 min at 37 $^\circ\text{C}$. (G) Fluorescence image, (H) bright-field image, and (I) the overlay image of HeLa cells treated with 20 $\mu\text{mol/L}$ CN^- in the growth media for 20 min at 25 $^\circ\text{C}$ and then incubated with **BFE** (10 $\mu\text{mol/L}$) for 30 min at 37 $^\circ\text{C}$. $\lambda_{\text{ex}}=404$ nm, collecting region: 450~550 nm, scale bar, 25 μm

3 Conclusions

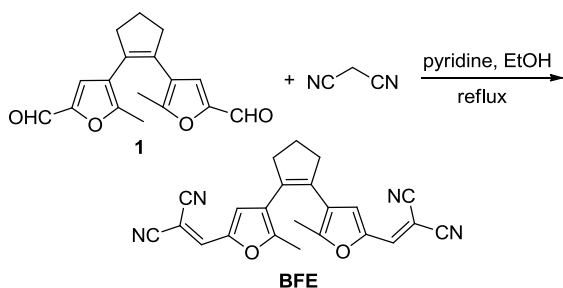
Herein, an efficient photoswitch **BFE** based on bisfurylenes has been developed. Compound **BFE** showed strong fluorescence whereas its analogue **BTE** did not display fluorescence due to the strong fluorescence derived from the superior furan to thiophene. In addition, its photochromic and fluorescent properties can be

modulated by cyanide ions, therefore, the photoswitch **BFE** can also act as a colorimetric and fluorescent probe for detecting cyanide ions. ^1H NMR titrations experiments were performed to explain the sensing mechanism of compound **BFE**, demonstrating that the nucleophilic addition of cyanide ions to the electrophilic carbon atom of the C=C bond of dicyano-vinyl group resulted in the suppression of the ICT effect in the molecule. Furthermore, high selectivity for cyanide ions and rapid fluorescent response to cyanide ions, enabled compound **BFE** to perform well in bioimaging application. This work provides a robust platform to develop photochromic probes with promising optical characteristics for fluorescent labeling techniques.

4 Experimental section

4.1 Materials and instrumentations

Compound **1** as shown in Scheme 3 was synthesized and purified according to the procedures published in the literature.^[30] All other reagents were used as received from commercial sources, unless specified otherwise, or prepared as described in the literature. All of the reactions were monitored by thin-layer chromatography (TLC) carried out on 0.25 mm Merck silica-gel (60-F254).



Scheme 3 Synthetic route of compound **BFE**

^1H NMR and ^{13}C NMR spectra were performed in CDCl_3 with TMS as internal standard on a Bruker Advance spectrometer at 400 MHz. High-resolution mass spectrometry (HR-MS) were recorded on a Thermo Fisher Scientific LTQ FTICR-MS spectrometer. UV-vis absorption spectra were recorded on a Shimadzu 1800 spectrophotometer and the fluorescent measurements were carried on a Jobin Yvon Fluorolog-3 spectrofluorometer (Model FL-TAU3). Both spectrophotometers were standardized. For the anion detection, each spectrum was acquired 2 min after anion addition. Absolute fluorescence quantum yields and fluorescence lifetimes were measured by horoba deltaflex 01 spectrometer.

4.2 Synthesis

Two drops of pyridine were added to the mixture of compound **1** (0.10 g, 0.352 mmol) and malononitrile (0.051 g, 0.775 mmol) in ethanol (10.0 mL). After refluxing for 4 h, the mixture was cooled to room temperature, and concentrated. Then the crude compound

was purified by silica gel column chromatography [$V(\text{petroleum ether}) : V(\text{ethyl acetate}) = 2 : 1$] to afford the compound **BFE** (0.113 g, 84.8%) as a yellow powder. m.p. 201~203 °C; ^1H NMR (400 MHz, CDCl_3) δ : 2.06~2.13 (m, 2H), 2.19 (s, 6H), 2.77 (t, $J=8.0$ Hz, 4H), 7.12 (s, 2H), 7.34 (s, 2H); ^{13}C NMR (100 MHz, CDCl_3) δ : 14.07, 22.52, 37.85, 75.76, 112.92, 114.08, 122.94, 124.18, 131.00, 141.99, 146.51, 151.71. HRMS (ESI⁺) calcd for $\text{C}_{23}\text{H}_{17}\text{O}_2\text{N}_4$ $[\text{M}+\text{H}]^+$ 381.1346, found 381.1345.

Supporting Information UV-vis absorption spectra of compound **BTE**, fluorescence spectra of compounds **BFE** and **BTE**, and characterization spectra of compounds **BFE**. The Supporting Information is available free of charge via the Internet at <http://sioc-journal.cn>.

References

- Grimm, J. B.; English, B. P.; Choi, H.; Muthusamy, A. K.; Mehl, B. P.; Dong, P.; Brown, T. A.; Lippincott-Schwartz, J.; Liu, Z.; Lionnet, T.; Lavis, L. D. *Nat. Methods* **2016**, *13*, 985.
- Zhao, F.; Chen, Z.; Fan, C. B.; Liu, G.; Pu, S. Z. *Dyes Pigm.* **2019**, *164*, 390.
- Yin, Y.; Zhao, F.; Chen, Z.; Liu, G.; Pu, S. Z. *Tetrahedron Lett.* **2018**, *59*, 4416.
- Tang, A. L.; Chen, Z.; Liu, G.; Pu, S. Z. *Tetrahedron Lett.* **2018**, *59*, 3600.
- Ju, Z. Y.; Shu, P. H.; Xie, Z. Y.; Jiang, Y. Q.; Tao, W. J.; Xu, Z. H. *Chin. J. Org. Chem.* **2019**, *39*, 697 (in Chinese). (鞠志宇, 舒朋华, 谢智宇, 蒋雨晴, 陶伟杰, 许志红, 有机化学, **2019**, *39*, 697.)
- Jiao, C. P.; Liu, Y. Y.; Lu, W. J.; Zhang, P. P.; Wang, Y. F. *Chin. J. Org. Chem.* **2019**, *39*, 591 (in Chinese). (娇春鹏, 刘媛媛, 路文娟, 张平平, 王延凤, 有机化学, **2019**, *39*, 591.)
- Li, Y. J.; Zhang, N.; Liu, J. H.; Jin, K.; Wang, S. Y. *Chin. J. Org. Chem.* **2018**, *38*, 3026 (in Chinese). (李英俊, 张楠, 刘季红, 靳焜, 王思远, 有机化学, **2018**, *38*, 3026.)
- Heim, R. *Nature* **1995**, *373*, 663.
- Dean, K. M.; Palmer, A. E. *Nat. Chem. Biol.* **2014**, *10*, 512.
- Xiong, Y.; Jentzsch, A. V.; Osterrieth, J. W. M.; Sezgin, E.; Sazanovich, I. V.; Reqlinski, K.; Galiani, S.; Parker, A. W.; Eggeling, C.; Anderson, H. L. *Chem. Sci.* **2018**, *9*, 3029.
- Eggeling, C.; Willig, K. I.; Sahl, S. J.; Hell, S. W. *Q. Rev. Biophys.* **2015**, *48*, 178.
- Betzig, E.; Patterson, G. H.; Sougrat, R.; Lindwasser, O. W.; Olenych, S.; Bonifacino, J. S.; Davidson, M. W.; Lippincott-Schwartz, J.; Hess, H. F. *Science* **2006**, *313*, 1642.
- Irie, M. *Chem. Rev.* **2000**, *100*, 1685.
- Fukaminato, T. *J. Photochem. Photobiol. C* **2011**, *12*, 177.
- Chen, S.; Chen, L. J.; Yang, H. B.; Tian, H.; Zhu, W. *J. Am. Chem. Soc.* **2012**, *134*, 13596.
- Pu, S. Z.; Sun, Q.; Fan, C. B.; Wang, R. J.; Liu, G. *J. Mater. Chem. C* **2016**, *4*, 3075.
- Cui, S. Q.; Qiu, S. Y.; Lu, R. M.; Pu, S. Z. *Tetrahedron Lett.* **2018**, *59*, 3365.
- Yun, C.; You, J.; Kim, J.; Huh, J.; Kim, E. *J. Photochem. Photobiol. C* **2009**, *10*, 111.
- Park, H.; Jin, Y. J.; Kwak, G. *Dyes Pigm.* **2017**, *146*, 398.
- Ritchie, C.; Vamvounis, G.; Soleimaninejad, H.; Smith, T. A.; Bieske, E. J.; Dryza, V. *Phys. Chem. Chem. Phys.* **2017**, *19*, 19984.
- Uno, K.; Niikura, H.; Morimoto, M.; Ishibashi, Y.; Miyasaka, H.; Irie, M. *J. Am. Chem. Soc.* **2011**, *133*, 13558.
- Roubinet, B.; Weber, M.; Shojaei, H.; Bates, M.; Bossi, M. L.; Be-

- lov, V. N.; Irie, M.; Hell, S. W. *J. Am. Chem. Soc.* **2017**, *139*, 6611.
- [23] Takagi, Y.; Morimoto, M.; Kashihara, R.; Fujinami, S.; Ito, S.; Miyasaka, H.; Irie, M. *Tetrahedron* **2017**, *73*, 4918.
- [24] Irie, M.; Mohri, M. *J. Org. Chem.* **1988**, *53*, 808.
- [25] Deng, X.; Liebeskind, L. S. *J. Am. Chem. Soc.* **2001**, *123*, 7703.
- [26] Yamaguchi, T.; Irie, M. *J. Mater. Chem.* **2006**, *16*, 4690.
- [27] Sysoiev, D.; Yushchenko, T.; Scheer, E.; Groth, U.; Steiner, U. E.; Exner, T. E.; Huhn, T. *Chem. Commun.* **2012**, *48*, 11355.
- [28] Sysoiev, D.; Fedoseev, A.; Kim, Y.; Boneberg, J.; Huhn, T.; Leiderer, P.; Scheer, E.; Groth, U.; Steiner, U. E. *Chem.-Eur. J.* **2011**, *17*, 6663.
- [29] Wolf, J.; Eberspächer, I.; Groth, U.; Huth, T. *J. Org. Chem.* **2013**, *78*, 8366.
- [30] Gidron, O.; Diskin-Posner, Y.; Bendikov, M. *J. Am. Chem. Soc.* **2010**, *132*, 2148.
- [31] Gidron, O.; Dadvand, A.; Sheynin, Y.; Bendikov, M.; Perepichka, D. F. *Chem. Commun.* **2011**, *47*, 1976.
- [32] Gidron, O.; Bendikov, M. *Angew. Chem., Int. Ed.* **2014**, *53*, 2546.
- [33] Zhao, Z.; Nie, H.; Ge, C.; Cai, Y.; Xiong, Y.; Qi, J.; Wu, W.; Kwok, R. T. K.; Gao, X.; Qin, A.; Lam, J. W. Y.; Tang, B. Z. *Adv. Sci.* **2017**, *4*, 1700005.
- [34] Gidron, O.; Dadvand, A.; Sun, E. W. H.; Chung, I.; Shimon, L. J. W.; Bendikov, M.; Perepichka, D. F. *J. Mater. Chem. C* **2013**, *1*, 4358.
- [35] Gidron, O.; Varsano, N.; Shimon, L. J. W.; Leitun, G.; Bendikov, M. *Chem. Commun.* **2013**, *49*, 6256.
- [36] Binder, J. B.; Raines, R. T. *J. Am. Chem. Soc.* **2009**, *131*, 1979.
- [37] Wang, S.; Zhou, Y.; Zhu, L.; Zhang, J.; Zou, Q.; Zeng, T.; Chen, W. *Chem. Commun.* **2017**, *53*, 9570.
- [38] Lucas, L. N.; Jong, J. J. D.; Esch, J. H.; Esch, J. H.; Kellogg, R. M.; Feringa, B. L. *Eur. J. Org. Chem.* **2003**, 155.
- [39] Li, W.; Jiao, C.; Li, X.; Xie, K.; Nakatani, K.; Tian, H.; Zhu, W. *Angew. Chem., Int. Ed.* **2014**, *53*, 4603.
- [40] Pati, P. B.; Zade, S. S. *RSC Adv.* **2013**, *3*, 13457.
- [41] Zhou, X.; Lv, X.; Hao, J.; Liu, D.; Guo, W. *Dyes Pigm.* **2012**, *95*, 168.
- [42] Lee, C. H.; Yoon, H. J.; Shim, J. S.; Jiang, W. D. *Chem.-Eur. J.* **2012**, *18*, 4513.
- [43] Yang, L.; Li, X.; Yang, J.; Qu, Y.; Hua, J. *ACS Appl. Mater. Interfaces* **2013**, *5*, 1317.
- [44] Zou, Q.; Li, X.; Xu, Q.; Ågren, H.; Zhao, W.; Qu, Y. *RSC Adv.* **2014**, *4*, 59809.

(Cheng, F.)